



Contents lists available at UGC-CARE

International Journal of Pharmaceutical Sciences and Drug Research

[ISSN: 0975-248X; CODEN (USA): IJPSPP]

journal home page : <https://ijpsdronline.com/index.php/journal>

Research Article

Natural Green Synthesis of Silver Nanoparticles Using Leaf Extract of *Guazuma ulmifolia* Lam. and Analysis of its Antimicrobial, Anti-inflammatory and Anticancer Activities

C Santhanakumar¹, A Vanitha^{2*}, VC Saralabai¹, K Kalimuthu³

¹PG and Research Department of Botany, Government Arts College (Autonomous), Coimbatore, Tamil Nadu, India.

²Department of Botany, Namakkal Kavignar Ramalingam Government Arts College for Women, Namakkal, Tamil Nadu, India.

³Department of Biotechnology, Dr. N.G.P Arts & Science College (Autonomous), Kalapatti, Coimbatore, Tamil Nadu, India.

ARTICLE INFO

Article history:

Received: 18 July, 2024

Revised: 08 August, 2024

Accepted: 11 September, 2024

Published: 30 September, 2024

Keywords:

Antibacterial, Anticancer, Anti-inflammatory, Cytotoxicity activities, *Guazuma ulmifolia*, Protein denaturation.

DOI:

10.25004/IJPSDR.2024.160509

ABSTRACT

Globally, silver nanoparticles (SNP) were created using a biologically activated green synthesis process that has raised substantial awareness of medical science and illness therapy. A new method of synthesizing SNPs based on a bottom-up, "green" approach is described here *Guazuma ulmifolia* Lam. leaf aqueous extract, in addition to assessing their antibacterial, anti-inflammatory, also anticancer *in-vitro* properties. By using the well diffusion method, the antibacterial activity possessed by nanoparticles against *Staphylococcus aureus*, *S. gallinarium*, *Bacillus subtilis*, *Pseudomonas stuberia*, in addition to *Escherichia coli* was examined. Subsequently, these *G. ulmifolia* silver nanoparticles (GUSNPs) were investigated for anticancer activity assessed by MTT assay utilizing HepG2 carcinoma cell line and anti-inflammatory activity assessed by HRBC stabilization assay protein denaturation assays. In dosage of 10 µg/mL, the GUSNPs had the maximum antibacterial activity against the following bacteria: *S. aureus* (7.1 mm), *S. gallinarium* (5.2 mm), *B. subtilis* (6.7 mm), *P. stuberia* (6.3 mm), and *E. coli* (4.7 mm), respectively. Membrane stabilization of HRBCs had a substantial anti-inflammatory activity (73.27 ± 0.89%), whereas the GUSNPs had the best protection of protein denaturation (79.35 ± 0.42%) at 1000 µg/mL. The best cytotoxicity activity of GUSNPs against HepG2 cell line was found in 500 µg/mL concentration with 24.32% of cell viability. The current study of GUSNPs has good antibacterial, anti-inflammatory, and anticancer activities

INTRODUCTION

Silver nanoparticles (SNPs) are distinguished by having the surface area to volume ratio must be high, and at least one dimension must be smaller than 100 nm. As a result of their outstanding antibacterial activity, the low thermal resistance and good optical properties of SNPs make them useful in a variety of industries, such as healthcare, food processing, environmental health, electronics, catalysis, and instrumental analysis.^[1] Biological approaches, which use plant extracts or living microbes, because of their simplicity and speed, have become increasingly popular in recent years, and cost-effectiveness.^[1,2] Plant extracts

have various advantages. First, plants are readily available and affordable. Second, unlike the SNPs are synthesized using plant extracts, which do not cause environmental damage. It has been shown that SNPs synthesized from plant extracts or pure phytochemicals possess antibacterial, antifungal, and antiviral functions,^[3] these anti-inflammatory,^[4] antioxidant,^[5,4] wound healing,^[6] anticancer,^[1,7] anticoagulant,^[8] cardioprotective,^[9] liver protective,^[9] antidiabetic,^[10] anti-cataractogenic,^[11] and anti-aging^[12] properties are all benefits of these compounds.

*Corresponding Author: Dr. A Vanitha

Address: Department of Botany, Namakkal Kavignar Ramalingam Government Arts College for Women, Namakkal, Tamil Nadu, India.

Email ✉: avanithagreen@gmail.com

Tel.: +91-9789408477

Relevant conflicts of interest/financial disclosures: The authors declare that the research was conducted in the absence of any commercial or financial relationships that could be construed as a potential conflict of interest.

© The Author(s) 2024. **Open Access.** This article is licensed under a Creative Commons Attribution 4.0 International License, which permits use, sharing, adaptation, distribution and reproduction in any medium or format, as long as you give appropriate credit to the original author(s) and the source, provide a link to the Creative Commons licence, and indicate if changes were made. The images or other third party material in this article are included in the article's Creative Commons licence, unless indicated otherwise in a credit line to the material. If material is not included in the article's Creative Commons licence and your intended use is not permitted by statutory regulation or exceeds the permitted use, you will need to obtain permission directly from the copyright holder. To view a copy of this licence, visit <https://creativecommons.org/licenses/by/4.0/>

SNPs have long been known to suppress numerous bacterial strains and pathogens found in medical and industrial operations.^[13] To prevent wound infection, certain lotions and topical ointments contain silver.^[14] Silver-doped polymers are also used in various surgical applications, such as dental implants.^[15] Additionally, consumer products containing silver a variety of sports equipment now contain silver-coated beads and colloidal silver gel.^[16]

As a result of external influences and chemical and physical stimulation, the body responds to inflammation. Otherwise, microbes enter the body, followed by a healing process. White blood cells and inflammatory tissue release various inflammatory mediators to ward off invasion and remove invading infections. As a result of excessive inflammation, reactive oxygen species and reactive nitrogen species accumulate, causing oxidative stress, cell damage, DNA damage, and contributing to diseases such as cancer, heart disease, and diabetes.^[17] Anti-inflammatory drugs, such as non-steroidal anti-inflammatory drugs (NSAIDs), are the two main types of medications used to treat inflammation. However, chronic NSAID use can lead to adverse effects such as liver and kidney damage, stomach inflammation, and the development of stomach ulcers.^[18] Thus, using plants that contain bioactive chemicals is one alternative to treating the inflammation of the skin.

A report by the World Health Organization (WHO) states, that among the most common types of cancer, liver cancer is one of the most common and will cause 830,000 deaths globally in 2020.^[19] Based on the results by Baloh *et al.*,^[20] in addition to cirrhosis and a high mortality rate, hepatocellular carcinoma (HCC) is the most common form of liver cancer. Thus, developing novel approaches to hepatic cancer treatment through nanotechnology is crucial, especially for plant-based nanomaterial therapy. *Guazuma ulmifolia* Lam. (Malvaceae) grows in Latin America, particularly Brazil and Mexico, and is also called mutamba and guacimo. The research was carried out among altitudes 384 plus 387 m, Latitude 21°43' S/Longitude 49° 3'. An experimental study going on ethnopharmacology has revealed that mutamba contains a wide spectrum of medicinal characteristics for its leaves, flowers, fruit, stem bark, and roots.^[21,22] The antibacterial, antioxidant, antiprotozoal, antidiarrheal, and cardioprotective properties of mutamba have been proven within and also *in-vitro*, *in-vivo* evaluations, substantiating its traditional applications. The primary secondary metabolites of this plant were also found to be phenolic compounds, particularly proanthocyanidins, aglycones, and glycosylated flavonoids, according to phytochemical investigations.^[23-26] Some countries prepare tea from dried leaves, which are then applied externally to treat bruises, rashes, and even bald spots. The tea is also used to treat kidney and digestive diseases, fever, diarrhea and diabetes. They apply a bark decoction

topically to treat skin diseases such as dermatosis, leprosy, and baldness.

The current study used *G. ulmifolia* Lam. aqueous leaf extract to create SNPs. These nanoparticles were characterized using UV spectroscopy, FTIR, XRD, SEM and EDX analysis. We tested the antibacterial, anti-inflammatory and anticancer activities of silver nanoparticles *in-vitro*.

MATERIALS AND METHODS

Leaf Extract Preparation of *G. ulmifolia*

G. ulmifolia leaves were shade-dry at room temperature and grind to a powder. About 500 mL of double-distilled water was combined with 100 g of the plant powder material, which was then extracted and heated for 20 to 30 minutes. The sample was normal filter through Whatman filter paper No. 1 to remove undissolved materials, such as cellular components and other components insoluble in the extraction solvent. After that, an extract was created. The extracted material was kept cold (4°C) in anticipation of future studies.^[27] After the extract add to petri dish and allowed to dry, a sterile blade was used to scrape it off. In preparation for more research, the plant powder was lastly kept in a light-sensitive amber vial.

Synthesis of Silver Nanoparticles by *G. ulmifolia* Leaf extract

Silver was extracted for the biosynthetic processes using 1-mM silver nitrate (AgNO₃) double distilled water solution. Leaf extract is mixed with silver nitrate in a 9:1 ratio. To form silver nanoparticles, *G. ulmifolia* plant aqueous extract of 10 and 90 mL AgNO₃ are combined. A magnetic stirrer running at 800 rpm was used to continuously stir the reaction mixture while it was heated below the boiling point at 70°C. The combination turned reddish brown after a day in a dark environment. Prior to being characterized, the nanoparticles were kept in a dark, dry, and cool atmosphere. By using UV spectroscopy, the color changes from green to brown during the formation of silver nanoparticles from plant extracts was verified.^[28]

Characterization of GUSNPs Nanoparticles

SNPs were confirmed through UV spectra, FTIR, XRD, SEM and EDX analysis.

UV-visible spectroscopy analysis

By reducing silver nanoparticles in solution might be seen through the Perkin-Elmer UV-VIS Spectrometer Lambda-35. At varied reaction rates of 200, 300, 400, 500, 600, 700, and 800 nm, in wavelength ranges from 200 to 800 nm, the solutions were scanned at 480 nm/min. The "UV Win lab" program was included with the spectrophotometer to capture and analyze data. A blank (distilled water) reference was used to adjust the spectrometer's baseline. The UV-visible spectrum of *G. ulmifolia* silver nanoparticles



(GUSNPs) and the information obtained were graphed. The reaction solution was incubated for several durations of 0, 1, 6, and 24 hours for each concentration (0.5, 1.0, 1.5, 2.0, 2.5, 3.0, 3.5). A study of the time-related impact of SNP production was conducted.

Fourier transform infrared analysis

Fourier transform infrared (FTIR) analysis was performed on the dried-out biomass of the extract after it was treated with AgNO₃ to explore and predict an interaction between different components of a formulation based on their physicochemical properties in order to determine the ingredient responsible for the creation of GUSNPs. The synthesized SNPs were subjected to FTIR measurements at 0, 6, 12, and 24 hours of reaction time. With samples to included KBr pellets, the FTIR Perkin Elmer tool, which has an absorption wavelength from 4000 to 400 cm⁻¹, was used to obtain the spectra. The results included a comparison of the functional peak shifts that can represent a specific molecular vibration. For example, a strong, sharp peak of approximately 4000 to 400 cm⁻¹.

X-ray diffraction analysis

This analysis was carried out by Rica Ku Ultima for the X-ray diffraction (XRD). An XRD technique and X-ray powder diffractometer were used to determine the crystal formation of the biosynthesized silver SNPs. Biologically studied using this technique the crystalline arrangement of SNPs formed. By applying the dispersion of SNPs resting on a glass slide with letting the ethanol solution evaporate, a thin layer of copper and silver nanoparticles was produced. X-ray diffraction was applied to this thin film a scanning haste of 2/min and an operating range of 10–80°.

Scanning electron microscopic analysis

Scanning electron microscopic (SEM) test was performed on GUSNPs with the Quanto 250 scanning electron microscope. A carbon-coated copper grid was used to generate thin films by simply dropping the sample onto it. The excess solution in the films was then collected with blotting paper, and a mercury lamp was used to dry the films above the SEM grid for five minutes.

Energy dispersive X-ray analysis

Utilizing energy dispersive X-ray (EDX) investigation located and confirmed to exist the elemental silver. The synthesized nanoparticles' arrangement was next investigated by drop-coating a very tiny quantity of the sample GUSNPs onto carbon film.^[29]

Antibacterial Activity of GUSNPs

The antibacterial activity of the GUSNPs sample was examined on five different bacterial species by means of the well diffusion method. For this investigation, five bacterial pathogens were utilized: 2 Gram-negative

bacteria (*Pseudomonas stutzeri* and *Escherichia coli*) and three gram-positive bacteria (*Bacillus subtilis*, *Staphylococcus nepalensis* and *S. aureus*). By two-fold dilution by 10 mg within 1-mL of sterilized double distilled water, concentrations of 10, 5, 2.5 mg, and 1.12 mg/mL were prepared. After, the culture was incubated at 37°C for 24 hours and bacterial culture inoculation using a nutrient agar medium for bacterial growth. Next, the inhibition zone was noted.

***In-vitro* Anti-Inflammatory Activity of GUSNPs**

Albumin denaturation assay inhibition

Using the suppression of albumin denaturation method, GUSNPs extract was evaluated for its anti-inflammatory effects.^[30,31]

- **Reagents**

5% Bovine serum albumin, 1N HCl, Phosphate buffer saline (pH-6.3).

- **Procedure**

This reaction mixture contains 0.5 mL of distilled water, 5% bovine serum albumin and 0.05 mL of bovine serum albumin. By adding 1 N HCl, the pH was raised to 6.3. Following a 20-minute incubation period at 37°C, varying volumes of plant extract were added 5 minutes heat treatment at 57°C was applied to the reaction mixture. Following cooling a phosphate buffer saline solution of 2.5 mL was added to the samples. Spectrophotometric measurements of turbidity were made at 600 nm. To determine the protein denaturation of percentage inhibition, the following formula was used:

$$\% \text{ Inhibition} = \frac{(\text{Abs}_{\text{Control}} - \text{Abs}_{\text{sample}})}{\text{Abs}_{\text{Control}}} \times 100$$

*HRBC membrane stabilization method*³²

Lysosomal enzymes secreted in the course of inflammation can induce a number of illnesses. It has been suggested that also chronic or acute inflammation is related to these enzymes of extracellular activity. Non-steroidal medicines function as non-steroidal agents because they inhibit lysosomal enzymes or stabilize lysosomal membranes.

- **Reagents**

Alsevers solution, 2% dextrose, 0.8% sodium citrate, 0.5% citric acid, 0.42% NaCl, 0.15M Phosphate buffer (pH 7.4), 0.36% Hypo saline, HRBC suspension (10% v/v)

- **Procedure**

After 2 mL of blood was extracted from healthy donors, equal parts of sterilised the Alsevers mixture were added and the mixture was centrifuged by 3000 rpm.

Before being used, in the packed cells, isosaline solution was used to clean them and 10% v/v saline was used to make a suspension. Both were then stored at 4°C without being disturbed. About 1-mL of phosphate buffer, 2 mL of hyposaline, and half a milliliter aspirin used as control (50, 100, 200, 500, and 1000 µg/mL), sterile distilled water (as an alternative of hypo saline to make 100% hemolysis), and 10% HRBC suspension were additional to the arranged mixture along with plant extracts (50, 100, 200, 500, and 1000 µg/mL) in common saline. Spectrophotometric measurements of the hemoglobin content of the supernatant solution were done by incubating every assay mixtures by 37°C for 30 minutes along with centrifuging the supernatant at 3000 rpm for 20 minutes. This formula can be used to determine the percentage of membrane stabilization in HRBCs:

$$\text{Percentage stabilization} = \frac{(\text{Abs}_{\text{Control}} - \text{Abs}_{\text{Sample}})}{\text{Abs}_{\text{Control}}} \times 100$$

In-vitro Anticancer Activity

MTT assay to determination of mitochondrial synthesis

- **Reagents**

Confluent monolayer cell cultures, TPVG solution, Dulbecco's modified Eagle's, medium (DMEM) with antibiotics, new born calf serum/sheep serum, microtitre plate (96 well), drug dilutions, MTT, prepared in Hanks balanced salt solution without phenol red, 2 mg/mL (HBSS-PR). (Sigma Chemicals), Propanol, Microplate reader (ELISA Reader, Bio-rad).

GUSNPs extract's anticancer activity *in-vitro* was investigated with the HepG2 cell line. Using DMEM media containing 10% FBS, 1.0×10^5 cells/mL were adjusted after centrifugation of the cell culture. A 96-well micro titre plate with a flat bottom was used, and 100 µL each well received a diluted cell suspension. After 24 hours to determine that the cell population is sufficient, 100 mL of diverse dilutions of the experiment samples created in the maintenance medium were introduced to the cells after they had been cleaned with phosphate buffer saline. Following a 48-hour incubation period at 37°C in a 5% CO₂ atmosphere, microscopic analysis was performed on the plates and observations were made every 24 hours. Following a 48-hour period, each well received 20 mL of MTT (2 mg/mL) in MEM-PR (MEM devoid of phenol red). The plates were incubated at 37°C in a 5% CO₂ environment for two hours after being gently shook. To dissolve the resulting formazan, add 100 mL of DMSO isopropanol and gently shake the plate. A microplate reader at 540 nm the absorbance was measured. Use the following formula to calculate the proportion of viable cells and use the dose-response curve to determine the numerical value of drug concentration and test sample concentration required to

inhibit growth of the cell by 50%.

$$\text{Percentage of inhibition (\%)} = \frac{\text{Control} - \text{Sample}}{\text{Control}} \times 100$$

Statistical Study

Mean ± SD values are the three independent extraction analyzes (n = 3). The IC₅₀ (effective half) of the different fractions from the antibacterial, anti-inflammatory and anticancer tests were analyzed using the ANOVA investigation, through a minimum difference of $p < 0.05$ as the level consequence.

RESULTS

Silver Nanoparticles Synthesis

The obtained leaf aqueous extract was placed in a Borosil Erlenmeyer flask of 500 mL on room temperature, sample added with 10 and 90 mL of 1M solution of silver nitrate within a 1:9 ratio (Fig. 1). A magnetic stirrer running at 800 rpm was used to continually stir the reaction mixture while it was heated below the boiling point of 60°C. The combination turned reddish brown after a day in a dark environment. Prior to being characterized, the nanoparticles were kept in a dark, dry, and cool atmosphere. By using a UV-visible spectroscope was used to measure the change from yellow-green to brown in color, and silver nanoparticles appearing from plant extract were verified (Fig. 1).

UV-visible Spectroscopy Analysis of GUSNPs Sample

A crucial characterization technique for studying nanoparticles is UV-vis analysis. A UV-vis spectrophotometer has been used to investigate the silver nitrate nanoparticles formed media of surface plasmon resonance (SPR). As a result of SPR excitation, visible light is absorbed by the nanoparticles, giving them different colors. UV-vis testing is performed on every sample of nanoparticles. Its UV-vis spectrum is displayed in Fig. 2. The peak absorption range for the produced nanoparticles was 300 to 800 nm.



A – Aqueous extract GU with AgNO₃ B - Mixture of plant extract with AgNO₃ after 24 hours

Fig. 1: Silver nanoparticles synthesis of *G. ulmifolia* plant leaves



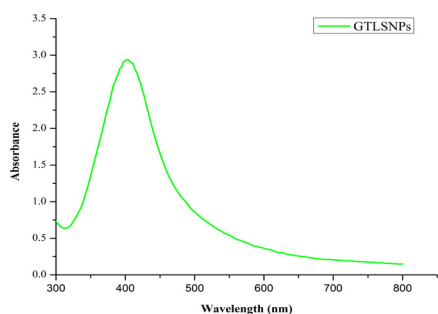


Fig. 2: UV- Visible spectroscopy analysis of GUSNPs sample

GUSNPs aqueous leaf extract had distinct bands of silver nitrate nanoparticles at a distance about 420 nm (Fig. 2).

FTIR Analysis of GUSNPs Sample

Using FTIR spectra, GUSNP aqueous leaf extract was analyzed. About 2 to 5 mL of the GUSNPs aqueous leaf extract sample were utilized for analysis. In the FTIR analysis, seven strong peaks were found. Certain functional groups were detected, including aromatics, aliphatic amines, phenols, aldehydes, and 1° amines (Table 1). The seven drop-down peaks 3295.7, 2935, 1591, 1382.1, 1044.2, 827.78, and 599.97, were noted. The following were noted: H, C-H stretching, N-H bend, C-C stretch, C-N stretch, C-Cl stretch, and C-Br stretch (Table 1 & Fig. 3).

Typical XRD Pattern of GUSNPs Sample

Four unique peaks with 2θ values were visible in the synthesized SNPs GU aqueous leaf extract has an X-ray diffraction pattern. 27.76, 32.12, 46.14, and 76.61° are the

Table 1: FTIR analysis of GUSNPs sample

S. No	Origin	Peak value	Functional group
1	H bonded	3295.7	Phenols
2	C-H stretching	2935	Aldehyde
3	N-H bend	1591	1° Amines
4	C-C stretch	1382.1	Aromatics
5	C-N stretch	1044.2	Aliphatic amines
6	C-Cl stretching	827.78	Halo compound
7	C-Br stretching	599.97	Halo compound

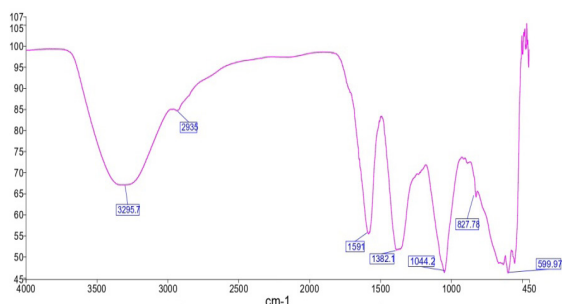


Fig. 3: FTIR analysis of GUSNPs sample

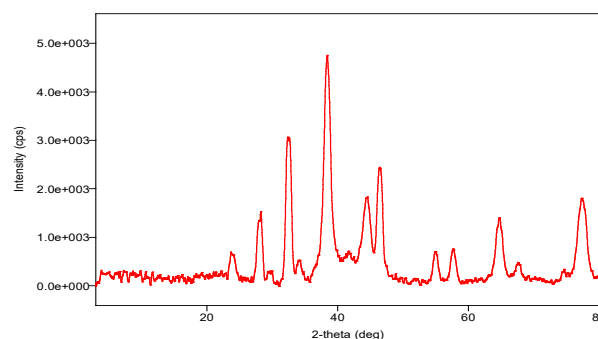


Fig. 4: Typical XRD pattern of GUSNPs sample

four values that were observed and can be viewed as sets of face-centered planes (100), (110), (200) and (622) (Fig. 4). The silver nanoparticles' face-centered cubic (FCC) lattice structure of these plane sets might be listed. The silver nanoparticles were calculated to have an average diameter of 240 nm using the Debye-Scherrer equation.

SEM Analysis of GUSNPs Sample

Find a better understanding of the scanning-reflective electron microscope using the shape and size of the resulting nanoparticles. Silver nanoparticles in individual aggregates as well as their quantity, were visible in the standard SEM picture. Silver nanoparticles had a morphology that was primarily spherical, aggregating into massive irregular structures with a lackluster appearance. Utilizing Image J software, the nanoparticles were quantified from the SEM picture. 240.83, 243.31, and 549.18 nm, respectively, were the silver nanoparticle sizes in SEM pictures of GUSNPs aqueous leaf extract (Fig. 5).

EDX Analysis of GUSNPs Sample

Qualitative and quantitative information on the chemical composition of SNPs evaluated by EDX analysis. A physically powerful signal for silver (Ag) on 3 keV the EDX spectrum of leaf extract of GUSNPs showed, confirming the production of SNPs. Other signals were detected for K, Cl, Na, O, Cu, and C, which are chemicals found in GUSNPs that act as capping agents (Fig. 6).

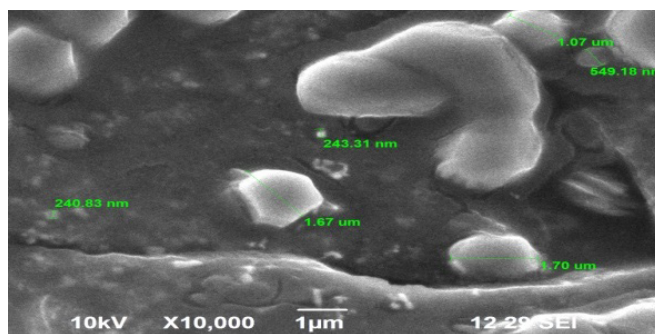


Fig. 5: SEM analysis of GUSNPs sample



Fig. 6: EDX analysis of GUSNPs sample

Antimicrobial Activity of GUSNPs Sample

GUSNPs produced by the filtrate and the antibacterial activity against *Staphylococcus aureus*, *S. gallinarium*, *Bacillus subtilis*, *Pseudomonas stuberia*, and *Escherichia coli* were shown to be good, with the maximum inhibitory zone. Green nanoparticle suspensions at various concentrations

were against gram-positive and gram-negative bacteria examined for antibacterial efficacy. The antimicrobial agent’s ability to rupture separate bacterial cells was assessed with the well diffusion method. Antibacterial effects against gram-positive bacteria and gram-negative bacteria were tested in various samples, as presented in Table 2.

Bacteria like *S. aureus*, *S. gallinarium*, *B. subtilis*, *P. stuberia*, and *E. coli* exhibit varying percentages of zone of inhibition at different concentrations (10, 05, and 2.5 µg/mL concentrations) (Table 2). *S. aureus*, *B. subtilis*, *P. stuberia*, *S. gallinarium*, *E. coli* and standard amoxicillin have an average percentage of inhibition of 7.1, 6.7, 6.3, 5.2, 4.7 and 13.8 mm at 10 µg/mL concentration (Table 2 & Plate 1). In this approach, the GUSNPs aqueous leaf extract demonstrates the inhibition zone of microorganisms. The best inhibition zone was identified at 10 µg/mL concentration in GUSNPs sample (Plate 1).

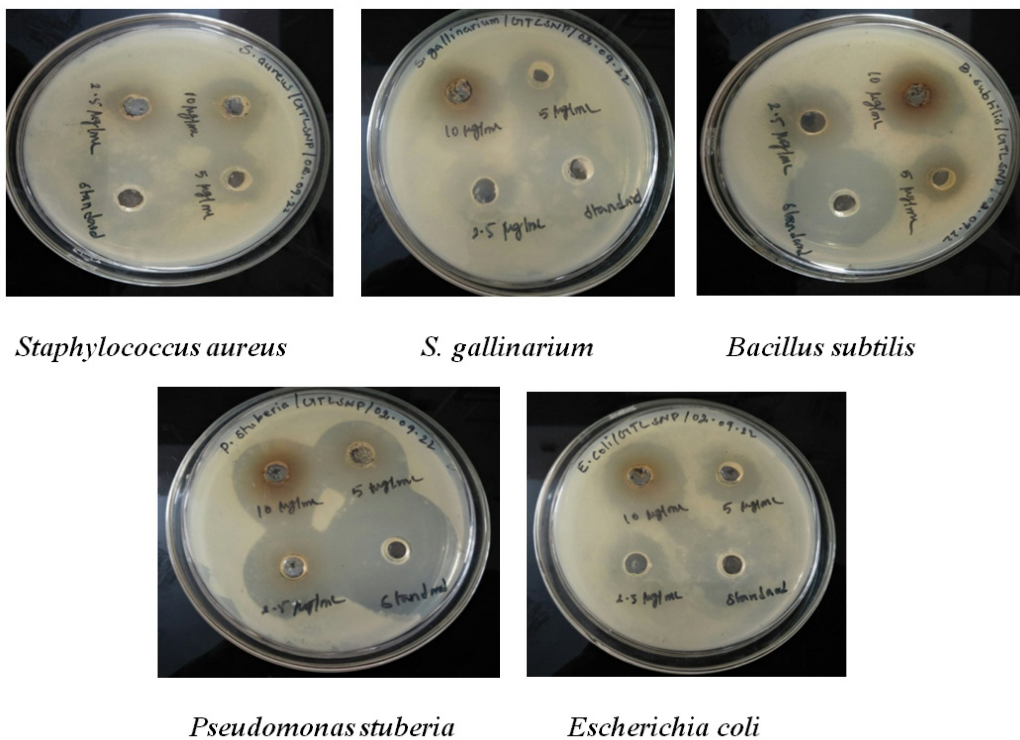


Plate 1: Antimicrobial activity of GUSNPs sample

Table 2: Antimicrobial activity of GUSNPs sample

S. No.	Organisms	Zone of inhibition (mm)			
		10 µg/mL	05 µg/mL	2.5 µg/mL	Standard (Amoxicillin)
1	<i>Staphylococcus aureus</i>	7.1	3.6	2.4	8.5
2	<i>S. gallinarium</i>	5.2	3.7	2.6	8.7
2	<i>Bacillus subtilis</i>	6.7	3.7	4.2	11.9
3	<i>Pseudomonas stuberia</i>	6.3	6.3	5.4	13.8
4	<i>Escherichia coli</i>	4.7	3.8	2.5	7.2



Table 3: Protein denaturation assay of GUSNPs sample

Samples	%of inhibition						
	1000 µg/mL	500 µg/mL	250 µg/mL	125 µg/mL	62.5 µg/mL	31.25 µg/mL	15.65 µg/mL
GUSNPs	79.35 ± 0.42	68.33 ± 0.23	57.71 ± 0.13	45.53 ± 0.76	35.73 ± 0.79	24.81 ± 0.83	17.33 ± 0.95
Aspirin	87.32 ± 0.27	76.17 ± 0.72	65.28 ± 0.89	54.59 ± 0.96	44.10 ± 0.98	33.15 ± 0.68	21.97 ± 0.22

Table 4: HRBC membrane stabilization assay of GUSNPs sample

Sample	% of inhibition						
	1000 µg/mL	500 µg/mL	250 µg/mL	125 µg/mL	62.5 µg/mL	31.25 µg/mL	15.65 µg/mL
GUSNPs	73.27 ± 0.89	62.26 ± 0.52	51.26 ± 0.15	42.47 ± 0.34	34.82 ± 0.03	25.52 ± 0.66	18.29 ± 0.99
Aspirin	85.32 ± 0.84	75.94 ± 0.04	64.71 ± 0.38	56.35 ± 0.69	47.31 ± 0.21	39.51 ± 0.92	30.31 ± 0.47

Anti-inflammatory Activity *In-vitro*

Protein denaturation assay of GUSNPs sample

The albumin denaturation inhibition assay of anti-inflammatory activity using GUSNP samples was assessed, to avoid protein denaturation which tests the capability of silver nanoparticles. GUSNPs were effective in inhibiting the degradation of albumin by heat at different doses (Table 3 and Fig. 7). Calculate the percent inhibition at 15.62, 31.25, 62.5, 125, 250, 500, and 1000 µg/mL extract concentrations. From the least concentration (15.62 µg/mL) to the uppermost concentration (1000 µg/mL), the percentage of inhibition ranged from 17.33 ± 0.95 to 24.81 ± 0.83, 35.73 ± 0.79, 45.53 ± 0.76, 57.71 ± 0.13, 68.33 ± 0.23, and 79.35 ± 0.42% (Table 3). The 50 percentage of inhibitory concentration (IC₅₀) was 214.72 µg/mL, while the control aspirin had an IC₅₀ of 87.32 µg/mL (Table 3). The findings indicate that GUSNPs were efficient at inhibiting heat-induced albumin denaturation. The bio-generated nanosilver showed a maximum inhibition of 79.35 ± 0.42% at 1000 µg/mL, showing its potential to prevent protein denaturation during inflammation (Fig. 7). This study suggests that the anti-inflammatory properties of nanoparticles are the result of a synergistic or individual effect of numerous phytochemical substances coated on the nanoparticles, such as naphthalene, hexadecanoic acid, and phytol.

HRBC membrane stabilization assay of GUSNPs sample

Table 4 shows the GUSNPs' anti-inflammatory activity results of as considered with the membrane stabilization experiment. Heat-induced hemolysis was inhibited at different extract concentrations. Samples were added to the HRBC mixture at 15.62, 31.25, 62.5, 125, 250, 500 and 1000 µg/mL concentrations, and the %hemolysis was correlated to control aspirin. At a dose of 1000 µg/mL, the greatest level of inhibition was found (Table 4). The sample had the highest anti-inflammatory activity (73.27 ± 0.89%), followed by 62.26 ± 0.52, 51.26 ± 0.15, 42.47 ± 0.34, 34.82 ± 0.035, 25.52 ± 0.66, and 18.29 ± 0.99% (Table 4

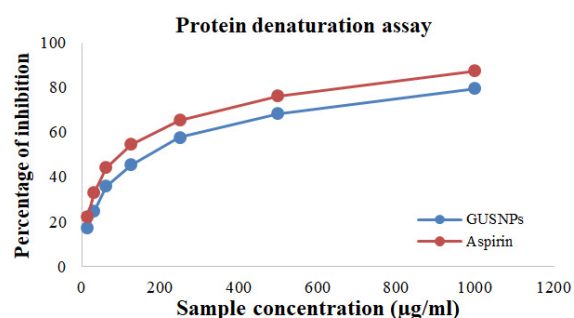


Fig. 7: Protein denaturation assay of GUSNPs sample

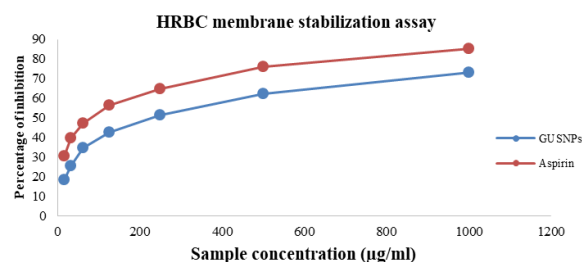


Fig. 8: HRBC membrane stabilization assay of GUSNPs sample

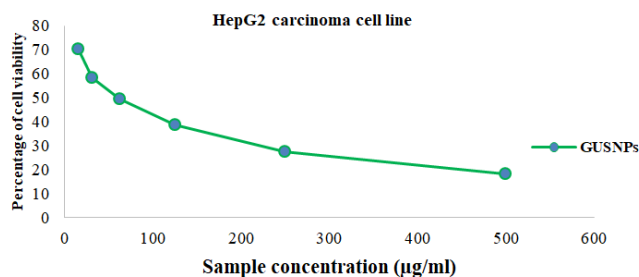
& Fig. 8). Its effectiveness as compared to regular aspirin was 85.32%. Table 4 and Fig. 8 show that the IC₅₀ values for GUSNPs and aspirin were 239.52 and 86.14 µg/mL, correspondingly.

Anticancer activity *in-vitro* of GUSNPs sample by 'HepG2 carcinoma cell line'

The cytotoxicity of silver nanoparticles containing GU was evaluated it was limited to different concentrations in the HepG2 cell line to determine the IC₅₀ values using the MTT assay. The sample is made at various concentrations (500, 400, 300, 200, and 100 µg/mL). GUSNPs had a significant influence on the HepG2 cell line at doses ranging since 500 to 100 µg/mL, according to an MTT test (Table 5 & Fig. 9). GUSNPs demonstrated the highest cytotoxicity next to the HepG2 cell line by a dosage of 500 µg/mL, with 24.32

Table 5: Anticancer activity *in-vitro* of GUSNPs sample by HepG2 carcinoma cell line

Sample	% of Inhibition					
	500 µg/mL	250 µg/mL	125 µg/mL	62.5 µg/mL	31.25 µg/mL	15.65 µg/mL
GUSNPs	70.20 ± 0.57	58.26 ± 1.7	49.34 ± 7.34	38.77 ± 7.46	27.60 ± 2.67	18.36 ± 9.95

**Fig. 9:** Anticancer activity *in-vitro* of GUSNPs sample by HepG2 carcinoma cell line

percent cell viability. Silver nanoparticles designed studies showed increased cell passage, with an IC₅₀ of 65.14 µg/mL (Table 5). Cell viability reduced as concentrations increased. Maximum cell death was found at 500 µg/mL concentration (Fig. 9).

DISCUSSION

A spectrophotometer's absorption spectra of the generated silver nanoparticles were used to confirm the colour shift of the aqueous extract including plants and metal salts, which signifies the combination of SNPs and Au-NPs.^[33] Under dark conditions, the current study's leaf aqueous extract turned reddish brown after just 24 hours. A dark, dry, and cool environment was used to preserve the nanoparticles prior to their characterization. UV-visible spectroscopy was used to confirm that plant extract had formed silver nanoparticles by observing a colour modify as of yellow green to brown. Related to this, Domany *et al.*^[34] and Ahmed *et al.*^[35] demonstrated similar findings, stating that the primary visual evidence of AgNPs synthesized with *Fusarium oxysporum* is visible by color change, indicating that Ag⁺ is reduced to Ag⁰ through the protein reducing agent contained in the fungal extract and metabolites.^[36]

A crucial characterisation technique for studying nanoparticles is UV-vis analysis. As a result of SPR excitation, visible light is absorbed by the nanoparticles, giving them different colors. UV-vis testing is performed on every sample of nanoparticles. GUSNPs aqueous leaf extract had distinct bands of silver nitrate nanoparticles at a distance of about 420 nm. In fresh leaves of *Guazuma ulmifolia* Lam, comparable outcomes were noted at 535 nm. According to Kartika *et al.*,^[33] the earlier publication, these results coincided. But the length of time it took to reduce depended on the temperature, pH, and bioactive components of the plant.^[37]

Utilizing FTIR analysis, the seven strong peaks were detected in the GUSNPs aqueous leaf extract. Halo compounds, aromatics, aliphatic amines, phenols, aldehydes, and 1° amines were among the functional groups that were detected. 3295.7, 2935, 1591, 1382.1, 1044.2, 827.78, and 599.97 are the seven drop-down peaks that were noted. N-H bend, C-C stretch, C-N stretch, C-Cl stretch, C-Br stretch, H, and C-H stretching were all noted. Based on research conducted by Zhang *et al.*,^[38] Niu *et al.*,^[39] You *et al.*,^[40] Luo *et al.*,^[41] and others, it appears that the FTIR absorbance band that is emerging it is associated with plant biological components such as protein, glucomannan, starch, saponin, colchicine, flavonoids, polysaccharides, phenylpropene and sugar.

Four unique peaks with 2θ values were visible in the synthesized SNP's GU aqueous leaf extract X-ray diffraction pattern. The following four numbers can be viewed as sets of face-centric planes: (100), (110), (200), and (622). These sets include 27.76, 32.12, 46.14, and 76.61°. These plane sets might be listed to the silver nanoparticles' face-centered cubic (FCC) lattice equation. 240 nm was determined to be calculation using the Debye-Scherrer equation the average size of silver nanoparticles was measured. The NP's amorphous crystalline structure is verified by XRD.^[42] Scanning electron microscopy offered further in order about the produced nanoparticles morphology and size features are produced. Shape of the silver nanoparticles is mostly spherical, and they are assembled into irregular structures with opaque regions morphologies. SEM scans revealed that green produced silver nanoparticles had a spherical form. SEM pictures GU aqueous leaf extract of silver nanoparticles were 240.83 nm, 243.31 nm, and 549.18 nm, in that order. The uniform distribution and compact size of the produced nanoparticles indicate that plant extract contains an adequate amount of reducing and stabilizing chemicals.^[43]

Both qualitative and quantitative details about the compound makeup of SNPs are provided by EDX analysis. The production of SNPs was confirmed by the metallic Ag at 3 keV strong signals in the EDX spectra of the GUSNPs aqueous leaf extract. For K, Cl, Na, O, Cu, and C compounds in GUSNPs serving as capping agents a number of additional signals were recorded. Determine the sample's elemental composition and purity as well as to validate that selenium ions were converted to elemental selenium were used EDX analysis.^[44] Pyrzynska and Sentkowska,^[45] have confirmed by the EDAX technology to the nanoparticles are made entirely of selenium and do not include any previous fundamental impurities.



In the current investigation, the greatest inhibitory zone of GUSNPs produced by the filtrate shown good antibacterial action beside *Staphylococcus aureus*, *S. gallinarium*, *Bacillus subtilis*, *Pseudomonas stuberia*, and *Escherichia coli*. Although it was initially discovered that using silver nanoparticles was more successful, chemical-based nanoparticles were later shown to have a harmful effect.^[46] As a result, researchers concentrated on creating non-toxic, economically viable, and environmentally benign nanoparticles using plant extract. Gram + and gram - bacteria were reduced towards suspensions of green synthesized nanoparticles at different concentrations to evaluate their antibacterial activity. The findings demonstrate that, in contrast as for gram + bacteria, gram - bacteria are more predisposed to nanoparticles.^[47] This may be brought on by the silver nanoparticles' electrostatic contact with that results in death of bacterial cell membrane.

The average percentage of inhibition of *S. aureus*, *B. subtilis*, *P. stuberia*, *S. gallinarium*, and *E. coli* bacteria is 7.1, 6.7, 6.3, 5.2 and 4.7 mm in the current experiment. Krishnaraj *et al.*^[48] reported to the SNPs generated as of the extract of *Acalypha indica* leaves had a particle size of 20 to 30 nm and a minimum inhibitory concentration (MIC) of 10 µg/mL when tested beside '*Escherichia coli* and *Vibrio cholera*'. During a different test,^[49] SNPs average size was produced by *Allium cepa* stem extract was 67 nm, and they demonstrated antibacterial efficacy against *Salmonella typhimurium* and *E. coli*. As a consequence of Kim *et al.*,^[50] Ag-NPs had a lowest amount inhibitory concentration of 100 µg/mL beside both *S. aureus* and *E. coli*. The zone of inhibition on the bacteria is thus demonstrated by the GUSNPs aqueous leaf extract. In the GUSNPs sample, the greatest zone of inhibition was noted at a dosage of 10 µg/mL. In accordance through Ruíz-Baltazar *et al.*,^[51] the standard element volume obtained from the extract of *Melissa officinalis* was 12 nm. They also noticed that silver nanoparticles with high control and anti-inflammatory properties next to *S. aureus* and *E. coli* could be produced using *Melissa officinalis*. Based on the reports, AgNPs can cling it attaches to the cell membrane of bacteria and enters the cytoplasm.^[52,53] These facts change the structure of the cells that destroy the organism.

GUSNPs a sample using the albumin denaturation test of anti-inflammatory activity was evaluated by testing the ability to prevent protein denaturation of silver nanoparticles. Through the activation of transcription factors like NF-KB, to control the generation of cytokines and the reactive oxygen species function as a mediator. This implies that other cytokines and ROS directly cause an seditious reaction.^[54,55] The similar results were observed in *Cadaba fruticosa* by JerunNisha *et al.*^[56] Control aspirin had an IC₅₀ value of 87.32 µg/mL with a 50 percent inhibitory concentration (IC₅₀) of 214.72 µg/mL. Many diseases are caused by lysosomal enzymes

that are released during inflammation, to be associated with acute or chronic inflammation and the extracellular activity of these enzymes is consideration. Consequently to Rajendran Vadivu and Lakshmi,^[57] non-steroidal medications work by either blocking these stabilizing the lysosomal membrane or lysosomal enzymes. At 1000 µg/mL, the maximum inhibition of 79.35 ± 0.42% was noted, demonstrating the bio-generated nano silver's ability to stop the denaturation of proteins implicated in the inflammatory process. It was shown that ethanol extracts decreased the amount of ROS production in cells. This study is consistent with other studies of *Pogostemon speciosus* Benth.,^[58] *Ceropegia juncea*,^[59] *Enteromorpha prolifera*.^[60] Flavonoids, a component of therapeutic plants that have been exposed to contain anti-inflammatory activities, have been found in ethanol extracts of *Hymenocallis littoralis*.^[61] Therefore, the individual or combined effects of different phytochemical components including naphthalene, hexadecanoic acid, and in this study, phytol coated on the nanoparticles may be the nanoparticles responsible for the anti-inflammatory properties.

Since the membrane of red blood cells (RBCs) is equivalent to the membrane of lysosomes and their stability indicates anti-inflammatory properties, the HRBC membrane stabilization technique was used.^[62] According to Yesmin *et al.*,^[63] the stability membrane of the lysosomal impedes the discharge of enzymes that induce irritation, hence preventing tissue injury and subsequent inflammation. Heat-induced hemolysis was inhibited by varying extract concentrations. 15.62, 31.25, 62.5, 125, 250, 500, and 1000 µg/mL concentrations of HRBC solution were added to each sample individually for incubation. The largest %of inhibitory was seen at 1000 µg/mL conc. Based on the results of Kumar *et al.*,^[64] the hypotonicity of the hyposaline in this study caused cell membrane lysis, the release of cell fluids, and the loss of electrolytes, all of which resulted in cell shrinkage. This in turn affected the hemolysis of RBC. The sample with the highest anti-inflammatory activity among them was 73.27 ± 0.89%; the next highest percentages were 62.26 ± 0.52, 51.26 ± 0.15, 42.47 ± 0.34, 34.82 ± 0.035, 25.52 ± 0.66, and 18.29 ± 0.99%, correspondingly. When compared to regular aspirin, it was 85.32%. By keeping the RBC membrane stable and limiting the discharge of lytic enzymes and previous seditious mediators, the plant extracts from *Solanum khasianum* demonstrated remarkable anti-inflammatory action. Ethanolic extract from the roots of *S. khasianum* had nearly identical efficacy to that of diclofenac. Still, a experiment of protein denaturation was second-hand before to report the anti-inflammatory efficacy *in-vitro* of *S. khasianum*'s fruit plus leaf methanolic extract.^[65] For both the aspirin and GUSNPs sample, the IC₅₀ value was initiate towards the 86.14 and 239.52 µg/mL. Previous reports in numerous Solanaceae species^[66-68] presented similar results of anti-inflammatory efficacy

with HRBC membrane stabilization method.

As a result of several studies^[69-71] the cytotoxicity of metal nanoparticles is related to a number of factors, including sizes, morphologies, and surface charges in addition to distinct biological resources providing reducing and capping agents. Within concentrations vary starting from 500 to 100 µg/mL, the MTT test of GUSNPs shows a significant effect on the HepG2 cell line. With 24.32% of cell viability, the 500 µg/mL concentration of GUSNPs demonstrated the strongest cytotoxicity action against the HepG2 cell line. With increasing convergence of silver nanoparticles-engineered tests, it was found that the level of cell passage increased, and the IC₅₀ was 65.14 µg/mL. The cell viability reduced as the concentration greater than before. In the maximum cell death was noted at the concentration of 500 µg/mL. The IC₅₀ standards (2.41 and 2.31 µg/mL⁻¹) intended for 'MCF-7 with HepG2 tumour cell lines' of SNPs produced as of the *Callisia fragrans* leaves aqueous extract hold small than to the IC₅₀ valuations of former plant extracts.^[72-74] The rationale is to *C. fragrans* leaf samples include lupeol and beta-amyrin. These compounds undergo a redox interaction by means of Ag⁺ atoms to produce lupenone and beta-amyrone, which are energetic chemicals by tremendous anticancer capabilities.^[75,76]

CONCLUSION

G. ulmifolia leaf SNPs are made sustainably and contain a selection of uses, including industrial and therapeutic, antimicrobial with anti-inflammatory applications. When silver ions are present, changes the colour to brown. The UV-vis, XRD, SEM, FTIR and EDAX analysis characterization was conducted. Analyzing the particle shape and size was done using SEM technology. The silver NPs' nature and particle size was measured using XRD. FTIR reported flavonoids also alkaline components. Beside the plant in addition carry out fine in the inhibitory zone through having antimicrobial qualities against bacteria. This study the plant *G. ulmifolia* a potent anti-inflammatory drug can be used as lead compound for designing gives on idea that the compound of which can be used for treatment of inflammation. Concentration-dependent cytotoxicity against HepG2 cancer cell lines from *G. ulmifolia*-mediated silver nanoparticles induced. Some new therapeutic agents for the cancer treatment has been evaluated as of *G. ulmifolia*-based SNPs. *G. ulmifolia* SNPs induced reactive oxygen species production and decreased the cell viability in HepG2 cell lines. Additional investigation can be conducted with common medications due to plants' to compare the effects of SNPs ability to inhibit environmental harm, used for treating these diseases. This medicinal plant showed positive results utilizing silver nanoparticles, a fast rising material in different fields and one of the innovations.

REFERENCES

- Islam MA, Jacob MV, Antunes EA. critical review on silver nanoparticles: From synthesis and applications to its mitigation through low-cost adsorption by biochar. *Journal of Environmental Management*. 2021;281:111918. Doi: 10.1016/j.jenvman.2020.111918.
- Beyene HD, Werkneh AA, Bezabh HK. Synthesis paradigm and applications of silver nanoparticles (AgNPs), a review. *Sustainable Mater Technology*. 2017;13:18–23. Doi: 10.1016/j.susmat.2017.08.001.
- Koduru JR, Kailasa SK, Bhamore JR, Kim KH, Dutta T, Vellingiri K. Phytochemical-assisted synthetic approaches for silver nanoparticles antimicrobial applications: A review. *Advanced Colloid Interface Science*. 2018;256:326–339. doi: 10.1016/j.cis.2018.03.001.
- Alkhalaf MI, Hussein RH, Hamza A. Green synthesis of silver nanoparticles by *Nigella sativa* extract alleviates diabetic neuropathy through anti-inflammatory and antioxidant effects. *Saudi Journal of Biological Science*. 2020;27:2410–2419. doi: 10.1016/j.sjbs.2020.05.005.
- Benedec D, Oniga I, Cuibus F, Sevastre, B, Stiufiuc G, Duma, M, *et al.* *Origanum vulgare* mediated green synthesis of biocompatible gold nanoparticles simultaneously possessing plasmonic, antioxidant and antimicrobial properties. *International Journal of Nanomedicine*. 2018;13:1041–1058. doi: 10.2147/IJN.S149819.
- Ravindran J, Arumugasamy V, Baskaran A. Wound healing effect of silver nanoparticles from *Tridax procumbens* leaf extracts on *Pangasius hypophthalmus*. *Wound Medicine journal*. 2019;27:100170. doi.org/10.1016/j.wndm.2019.100170.
- Rajan R, Chandran K, Harper SL, Yun SI, Kalaichelvan PT. Plant extract synthesized nanoparticles: An ongoing source of novel biocompatible materials. *Industrial Crops Production*. 2015;70:356–373. DOI:10.1016/j.indcrop.2015.03.015.
- Asghar MA, Yousuf RI, Shoaib MH, Asghar MA. Antibacterial, anticoagulant and cytotoxic evaluation of biocompatible nanocomposite of chitosan loaded green synthesized bioinspired silver nanoparticles. *International Journal of Biological Macromolecules*. 2020;160:934–943. doi: 10.1016/j.ijbiomac.2020.05.197.
- Ali MS, Anuradha V, Yogananth N, Krishnakumar S. Heart and liver regeneration in zebrafish using silver nanoparticles synthesized from *Turbinaria conoides*-*In vivo*. *Biocatalytic and Agricultural Biotechnology*. 2019;17:104–109.
- Jini D, Sharmila S. Green synthesis of silver nanoparticles from *Allium cepa* and its *in-vitro* antidiabetic activity. *Mater Today Process*. 2020;22:432–438. doi.org/10.1016/j.matpr.2019.07.672.
- Anbukkarasi M, Thomas PA, Teresa PA, Anand T, Geraldine P. Comparison of the efficacy of a *Tabernaemontana divaricata* extract and of biosynthesized silver nanoparticles in preventing cataract formation in an *in vivo* system of selenite-induced cataractogenesis. *Biocatalytic and Agricultural Biotechnology*. 2020;23:101475. DOI:10.1016/j.bcab.2019.101475.
- Radwan RA, El-Sherif YA, Salama MM. A novel biochemical study of anti-ageing potential of *Eucalyptus camaldulensis* bark waste standardized extract and silver nanoparticles. *Colloids Surface B Biointerface*. 2020;191:111004. doi: 10.1016/j.colsurfb.2020.111004.
- Jiang H, Manolache S, Wong ACL, Denes FS. Plasma-enhanced deposition of silver nanoparticles onto polymer and metal surfaces for the generation of antimicrobial characteristics. *Journal of Applied Pollution Science*. 2004;93(3):1411–1422. DOI:10.1002/app.20561.
- Becker RO. Silver ions in the treatment of local infections. *Metal-based drugs*. 1999;6(4-5):311–14. doi: 10.1155/MBD.1999.311.
- Silver S. Bacterial silver resistance: molecular biology and uses and misuses of silver compounds. *FEMS Microbiological Review*. 2003;27(2-3):341–53. doi: 10.1016/S0168-6445(03)00047-0.
- Song JY, Kim BS. Rapid biological synthesis of silver nanoparticles



- using plant leaf extracts. *Bioprocess Biosystems and Engineering*. 2009;32(1):79-84. doi: 10.1007/s00449-008-0224-6.
17. Pizzino G, Irrera N, Cucinotta M, Pallio G, Mannino F, Arcoraci V, *et al.* Oxidative Stress: Harms and Benefits for Human Health. *Oxidative Medicinal Cellulose Long*. 2017;2020:1-13. doi: 10.1155/2017/8416763.
 18. Harirforoosh S, Asghar W, Jamali F. Adverse Effects of Non-steroidal Anti-inflammatory Drugs: An Update of Gastrointestinal, Cardiovascular and Renal Complications. *Journal of Pharmacy and Pharmaceutical Science*. 2013;16(5):821-847. doi: 10.18433/j3vw2f.
 19. Adegbola O, Ajayi GO. Screening for gestational diabetes mellitus in Nigerian pregnant women using fifty-gram oral glucose challenge test. *West African Journal of Medicine*. 2008;27:139-143.
 20. Balogh J, Victor III D, Asham EH, Burroughs SG, Boktour M, Saharia A, *et al.* Hepatocellular carcinoma: a review. *Journal of hepatic Cardio*. 2016;41-53. doi: 10.2147/JHC.S61146.
 21. Al Muqarrabun L MR, Ahmat N. Medicinal uses, phytochemistry and pharmacology of family Sterculiaceae: a review. *Euro. Journal of Medicinal Chemistry*. 2015;92:514-530. doi: 10.1016/j.ejmech.2015.01.026.
 22. Navarro V, Villarreal ML, Rojas G, Lozoya X. Antimicrobial evaluation of some plants used in Mexican traditional medicine for the treatment of infectious diseases. *Journal of Ethnopharmacology*. 1996;53(3):143-147. doi: 10.1016/0378-8741(96)01429-8.
 23. Assis RQ, Andrade KL, Gomes Batista LE, de Oliveira Rios A, Dias DR, Ndiaye EA, *et al.* Characterization of mutamba (*Guazuma ulmifolia* LAM.) fruit flour and development of bread. *Biocatalytic and Agricultural Biotechnology*. 2019;19:101120. Doi: 10.1016/j.BCAB.2019.101120.
 24. dos Santos JM, Alfredo TM, Antunes KA, da Cunha J, ... de Picoli Souza K. *Guazuma ulmifolia* Lam. Decreases oxidative stress in blood cells and prevents doxorubicin-induced cardiotoxicity. *Oxida. Medical and Cellular Long*. 2018;2018:1-16. doi: 10.1155/2018/2935051.
 25. Hor M, Heinrich M, Rimpler H. Proanthocyanidin polymers with antisecretory activity and proanthocyanidin oligomers from *Guazuma ulmifolia* bark. *Phytochemistry*. 1996;42(1):109-119. doi: 10.1016/0031-9422(95)00855-1.
 26. Hor M, Rimpler H, Heinrich M. Inhibition of Intestinal Chloride Secretion by Proanthocyanidins from *Guazuma ulmifolia*. *Planta and Medical*. 1995;61(03):208-212. doi: 10.1055/s-2006-958057.
 27. Subramaniam P, Nisha KJ, Vanitha A, Kiruthika ML, Sindhu P, Elesawy BH, *et al.* Synthesis of silver nanoparticles from wild and tissue cultured *Ceropegia juncea* plants and its antibacterial, anti-angiogenesis and cytotoxic activities. *Applied Nanoscience*. 2021;1-15. Doi: 10.1007/s13204-021-02092-z.
 28. Sankar R, Maheswari R, Karthik S, Shivashangari KS, Ravikumar V. Anticancer activity of *Ficus religiosa* engineered copper oxide nanoparticles. *Mater Science and Engineering. C*. 2014;44:234-239. doi: 10.1016/j.msec.2014.08.030.
 29. Vigneshwaran N, Ashtaputre NM, Varadarajan PV, Nachane RP, Paralakar KM, Balasubramanyan RH. Biological synthesis of silver nanoparticles using the fungus *Aspergillus flavus*. *Mater Letters*. 2007;61:1413-8. http://dx.doi.org/10.1016/j.matlet.2006.07.042.
 30. Mizushima Y, Kobayashi M. Interaction of anti-inflammatory drugs with serum proteins, especially with some biologically active proteins. *Journal of Pharmacy and Pharmaceutical*. 1968;20(3):169-173. doi: 10.1111/j.2042-7158.1968.tb09718.x.
 31. Sakat S, Juvekar AR, Gambhire MN. In-vitro antioxidant and anti-inflammatory activity of methanol extract of *Oxalis corniculata* Linn. *Inter. Journal of Pharmacy and Pharmaceutical Science*. 2010;2(1):146-155. DOI:10.1055/s-0029-1234983.
 32. Kumar V, Bhat ZA, Kumar D, Bohra P, Sheela S. *In-vitro* anti-inflammatory activity of leaf extracts of *Basella alba* linn. var. *alba*. *Inter. Journal of Drug Development and Research*. 2011;3(2):176-179.
 33. Karthika V, Arumugam A, Gopinath K, Kaleeswarran P, Govindarajan M, Alharbi NS, *et al.* *Guazuma ulmifolia* bark-synthesized Ag, Au and Ag/Au alloy nanoparticles: Photocatalytic potential, DNA/protein interactions, anticancer activity and toxicity against 14 species of microbial pathogens. *Journal of Photochemistry and Photobiology B: Bioscience*. 2017;167:189-199. https://doi.org/10.1016/j.jphotobiol.2017.01.008.
 34. El Domany BE, Tamer ME, Amr EA, Ahmed AF. Biosynthesis, Characterization, Antibacterial and Synergistic Effect of Silver Nanoparticles using *Fusarium oxysporum*. *Journal of Pure Applied Micro-biology*. 2017;11(3):1441-1446. https://doi.org/10.22207/JPAM.11.3.27.
 35. Ahmed AA, Haider H, Mohammed M. Analyzing formation of silver nanoparticles from the filamentous fungus *Fusarium oxysporum* and their antimicrobial activity. *Turkey Journal of Bioscience*. 2018;42:54-62. doi: 10.3906/biy-1710-2.
 36. Costa Silva LP, Oliveira JP, Keijok WJ, da Silva AR, Aguiar AR, Guimaraes MC, *et al.* Extracellular biosynthesis of silver nanoparticles using the cell-free filtrate of nematophagous fungus *Duddingtonia flagrans*. *International Journal of Nanoscience*. 2017;12:6373-6381. doi: 10.2147/IJN.S137703.
 37. Kajani A, Bordbar AK, Esfahani SHZ, Khosropour AR, Razmjou A. Green synthesis of anisotropic silver nanoparticles with potent anticancer activity using *Taxus baccata* extract. *RSC Advances journal*. 2014;4:61394-61403. DOI: 10.1039/C4RA08758E.
 38. Zhang T, Gao J, Jin ZY, Xu XM, Chen HQ. Protective effects of polysaccharides from *Lilium lancifolium* on streptozotocin-induced diabetic mice. *Inter J bio Macro*. 2014;65:436-440. doi: 10.1016/j.ijbiomac.2014.01.063.
 39. Niu LX, Li ZN, Li HJ, Zhang YL. Study on ultrasonic wave extraction of flavonoids from the bulb of *Lilium lancifolium*. *Zhong yao cai= Zhongyao cai= Journal of Chin Medical and Mate*, 2007;30(1):85-88.
 40. You X, Xie C, Liu K, Gu Z. Isolation of non-starch polysaccharides from bulb of tiger lily (*Lilium lancifolium* Thunb.) with fermentation of *Saccharomyces cerevisiae*. *Carbohydrate and Polymers*. 2010;81(1):35-40. DOI: 10.1016/j.carbpol.2010.01.051.
 41. Luo J, Li L, Kong L. Preparative separation of phenylpropanoid glycerides from the bulbs of *Lilium lancifolium* by high-speed counter-current chromatography and evaluation of their antioxidant activities. *Food Chemistry*. 2012;131(3):1056-1062. DOI:10.1016/j.foodchem.2011.09.112.
 42. Langi Bhushan, Shah Chetan, Singh, Krishan Kant, Chaskar, Atul, *et al.* "Ionic liquid-induced synthesis of selenium nanoparticles," *Mater Research and Bullets*. 2012;45:668.
 43. Ahmad T, Bustam MA, Irfan M, Moniruzzaman M, Asghar HMA, Bhattacharjee S. Green synthesis of stabilized spherical shaped gold nanoparticles using novel aqueous *Elaeis guineensis* (oil palm) leaves extract. *Journal of molecular and Structure*. 2018;1159:167-173. DOI: 10.1016/j.molstruc.2017.11.095.
 44. Ingole AR, Thakar SR, Khati NT, Wankhade AV, Burghate DK. "Green synthesis of selenium nanoparticles under ambient condition". *Chalcogenide Letters*. 2010; 7:485-489.
 45. Pyrzynska K, Sentkowska A. "Biosynthesis of selenium nanoparticles using plant extracts," *Journal of Nanostructure and Chemistry*. 2021;1-14. https://doi.org/10.1007/s40097-021-00435-4.
 46. Ahmad K, Warsito B, Hidayat JW, Khan S, Ahmed N, Calvin EJ, *et al.* Green synthesis of silver nanoparticles and degradation of AZO-dyes using *Cestrum diurnum* plant extract, and antimicrobial activities of AgNP's. *Journal of Bioremedial and Environmetal Science*. 2023;2(2):78-88. DOI: 10.14710/jbes.2023.19246.
 47. Abbaszadegan A, Ghahramani Y, Gholami A, Hemmateenejad B, Dorostkar S, Nabavizadeh M, *et al.* The effect of charge at the surface of silver nanoparticles on antimicrobial activity against gram-positive and gram-negative bacteria: a preliminary study. *Journal of Nanoscience*. 2015;16(1):53-53. DOI: 10.1155/2015/720654.
 48. Krishnaraj C, Jagan E, Rajasekar S, Selvakumar P, Kalaichelvan PT, Mohan NJCSBB. Synthesis of silver nanoparticles using *Acalypha indica* leaf extracts and its antibacterial activity against water borne pathogens. *Colloids Surface B Biointerface*. 2010;76(1):50-56. doi: 10.1016/j.colsurfb.2009.10.008.
 49. Balamanikandan T, Balaji S, Pandiarajan J. Biological synthesis of silver nanoparticles by using onion (*Allium cepa*) extract and their antibacterial and antifungal activity. *World Applied Science*

- Journal. 2015;33:939-43. DOI: 10.5829/idosi.wasj.2015.33.06.9525.
50. Kim SH, Lee HS, Ryu DS, Choi SJ, Lee DS. Antibacterial activity of silver-nanoparticles against *Staphylococcus aureus* and *Escherichia coli*. Korean Journal of Microbiology and Biotechnology. 2011;39(1):77-85.
 51. de Jesús Ruíz-Baltazar Á, Reyes-López SY, Larrañaga D, Estévez M, Pérez R. Green synthesis of silver nanoparticles using a *Melissa officinalis* leaf extract with antibacterial properties. Results Physiology. 2017;7:2639-43. Doi: 10.1016/j.rinp.2017.07.044.
 52. Pazos-Ortiz E, Roque-Ruiz JH, Hinojos-Márquez EA, López-Esparza J, Donohué-Cornejo A, Cuevas-González JC, *et al.* Dose-dependent antimicrobial activity of silver nanoparticles on polycaprolactone fibers against Gram-positive and Gram-negative Bacteria. Journal of Nanomaterials. 2017;2017(1). DOI:10.1155/2017/4752314.
 53. López-Esparza J, Espinosa-Cristóbal LF, Donohue-Cornejo A, Reyes-López SY. Antimicrobial activity of silver nanoparticles in polycaprolactone nanofibers against gram-positive and gram-negative bacteria. Industrial Engineering and Chemical Research. 2016;55(49):12532-12538.
 54. Ilavarasan R, Mallika M, Venkataraman S. "Anti-inflammatory and free radical scavenging activity of *Ricinus communis* root extract," Journal of Ethnopharmacological. 2006;103:478-480. doi: 10.1016/j.jep.2005.07.029.
 55. Saini AK, Goyal R, Gauttam VK, Kalia AN. "Evaluation of anti-inflammatory potential of *Ricinus communis* Linn. leaves extracts and its flavonoids content in Wistar rats," Journal of Chemistry and Pharmaceutical Research. 2010;2:690-695. DOI:10.1186/s13104-017-3001-2.
 56. JerunNisha KM, Vanitha A, Kiruthika ML, Viswanathan P, Kalimuthu K. Biosynthesis of Silver and Copper Nanoparticles Using *Cadaba fruticosa* (L.) Druce and its Biological Applications. Asian Pacific Journal of Health Sciences. 2021;8:1-12. DOI: <https://doi.org/10.21276/apjhs.2021.8.3.12>.
 57. Rajendran Vadivu, Lakshmi KS. *In-vitro* and *in vivo* anti inflammatory activity of leaves of *Symplocos cochinchinensis* (Lour) Moore ssp *Laurina*. Bangladesh Journal of Pharmacology. 2008;3:121-124. DOI: <https://doi.org/10.3329/bjp.v3i2.956>.
 58. Sathiyasheela D, Viswanathan P, Kalimuthu K, Vanitha A. Facile synthesis of silver nanoparticles, anti-inflammatory, antibacterial and photocatalytic activities using *Pogostemon speciosus* Benth. An endemic medicinal plant. Journal of Water and Environmental Nanotechnology. 2022;7:306-316. <https://doi.org/10.22090/jwent.2022.03.006>.
 59. Subramaniam P, Vanitha A, Kalimuthu K, Sathiyasheela D, ShanthiPriya E. Phytosynthesis of copper nanoparticles using wild *Ceropegia juncea* and its therapeutic activities. Research Journal of Agricultural Sciences. 2022;13:1024-1031.
 60. Kingslin A, Kalimuthu K, Kiruthika ML, Khalifa AS, Nhat PT, Brindhadevi K. Synthesis, characterization and biological potential of silver nanoparticles using *Enteromorpha prolifera* algal extract. Applied Nanoscience. 2022;1-14. DOI: 10.1007/s13204-021-02105-x.
 61. Taur DJ, Waghmare MG, Bandal RS, Patil RY. "Antinociceptive activity of *Ricinus communis* L. leaves," Asian Pacific Journal of Tropical Biomedicine. 2011;1:139-141. doi: 10.1016/S2221-1691(11)60012-9.
 62. Chou CT. The Anti-inflammatory effect of an extract of *Tripterygium wilfordii* Hook F on adjuvant-induced paw oedema in rats and inflammatory mediators release. Phytother Research. 1997;11(2):152-154. DOI:10.1002/(SICI)1099-1573(199703)11:2<152::AID-PTR45>3.0.CO;2-L.
 63. Yesmin S, Paul A, Naz T, Rahman AA, Akhter SF, Wahed MI, Emran TB, Siddiqui SA. Membrane stabilization as a mechanism of the anti-inflammatory activity of ethanolic root extract of Choi (*Piper chaba*). Clinical Phytoscience. 2020;6(1):1-10. DOI: <https://doi.org/10.1186/s40816-020-00207-7>.
 64. Kumar V, Bhat ZA, Kumar D, Bohra P, Sheela S. *In-vitro* anti-inflammatory activity of leaf extracts of *Basella alba* linn. Var. *alba*. International Journal of Drug Development and Research. 2011;3(2):176-179.
 65. Gogoi R, Sarma N, Pandey SK, Lal M. Phytochemical constituents and pharmacological potential of *Solanum khasianum* CB Clarke. extracts: Special emphasis on its skin whitening, antidiabetic, acetylcholinesterase and genotoxic activities. Trends Phytochemistry and Research. 2021;5(2):47-61. DOI:10.30495/TPR.2021.1917249.1190.
 66. Pungle R, Tambe A, More A, Kharat A. Anti-inflammatory and antioxidant potentiality of *Solanum xanthocarpum*. Africal Journal of Biotechnology. 2018;17(37):1188-1195. DOI:10.5897/AJB2018.16560.
 67. Gupta S. *In-Vitro* anti-inflammatory activity of *S. xanthocarpum* and *A. officinarum* herb by human red blood cell membrane stabilization method. Journal of Drug Delivery and Therapeutics. 2019;9(3):663-666. DOI: <https://doi.org/10.22270/jddt.v9i3-s.2948>.
 68. Kavitha R, Ringley CM, Salomy SR, Piramila BH, Rose AF. *In-vitro* analysis of antidiabetic and anti-inflammatory activities of selected medicinal plants. Journal of Pharmaceutical Science and Research. 2021;13(5):259-270.
 69. Mostafavi E, Zarepour A, Barabadi H, Zarrabi A, Truong BL, Medina-Cruz D. Antineoplastic activity of biogenic silver and gold nanoparticles to combat leukemia: beginning a new era in cancer theragnostic. Biotechnology Represents. 2022;34:e00714. DOI:10.1016/j.btre.2022.e00714.
 70. Virmani I, Sasi C, Priyadarshini E, Kumar R, Sharma KS, Singh PG, Meena R. Comparative anticancer potential of biologically and chemically synthesized gold nanoparticles. Journal of Cluster Science. 2020;31:867-76. DOI:10.1007/s10876-019-01695-5.
 71. Barabadi H, Vahidi H, Mahjoub AM, Kosar Z, Kamali DK, Ponmurugan K, *et al.* Emerging antineoplastic gold nanomaterials for cervical cancer therapeutics: a systematic review. Journal of Cluster Science. 2020;31:1173-1184. doi: 10.2147/IJN.S240293.
 72. Alahmad A, Feldhoff A, Bigall NC, Rusch P, Scheper T. *Hypericum perforatum* L.-mediated green synthesis of silver nanoparticles exhibiting antioxidant and anticancer activities. Nanomaterials. 2021;11:487. <https://doi.org/10.3390/nano11020487>.
 73. Patra JK, Das G, Shin HS. Facile green biosynthesis of silver nanoparticles using *Pisum sativum* L. outer peel aqueous extract and its antidiabetic, cytotoxicity, antioxidant, and antibacterial activity. International Journal of Nanomedicine. 2019;14:6679-90. DOI <https://doi.org/10.2147/IJN.S212614>.
 74. Hashemi Z, Mizwari ZM, Mohammadi-Aghdam S, Mortazavi-Derazkola S, Ebrahimzadeh MA. Sustainable green synthesis of silver nanoparticles using *Sambucus ebulus* phenolic extract: optimization and assessment of photocatalytic degradation of methyl orange and there *in-vitro* antibacterial and anticancer activity. Arabian Journal of Chemistry. 2022;15:103525. <https://doi.org/10.1016/j.arabjc.2021.103525>.
 75. Almeida PDO, Boleti APA, Rüdiger AL, Lourenço GA, Veiga Junior VF, Lima, ES. Anti-inflammatory activity of triterpenes isolated from *Protium paniculatum* oil-resins. Evidence-Based Complement Alter Medicine. 2015;10:293768. doi: 10.1155/2015/293768.
 76. Ferreira RGS, Silva Júnior WF, Veiga Junior VF, Lima AAN, Lima ES. Physicochemical characterization and biological activities of the triterpenic mixture α , β -amyrenone. Molecules. 2017;22:298. <https://doi.org/10.3390/molecules22020298>.

HOW TO CITE THIS ARTICLE: Santhanakumar C, Vanitha A, Saralabai VC, Kalimuthu K. Natural Green Synthesis of Silver Nanoparticles Using Leaf Extract of *Guazuma ulmifolia* Lam. and Analysis of its Antimicrobial, Anti-inflammatory and Anticancer Activities. Int. J. Pharm. Sci. Drug Res. 2024;16(5):813-824. DOI: 10.25004/IJPSDR.2024.160509

